Published in final edited form as:
*J Am Chem Soc*. 2011 November 16; 133(45): 18280–18288. doi:10.1021/ja2064389.

# Iterative *In situ* Click Chemistry Assembles a Branched Capture Agent and Allosteric Inhibitor for Akt1

**Steven W. Millward**, **Ryan K. Henning**, **Gabriel A. Kwong**[†], **Suresh Pitram**[‡], **Heather D. Agnew**[‡], **Kaycie M. Deyle**, **Arundhati Nag**, **Jason Hein**[§], **Su Seong Lee**[1], **Jaehong Lim**[1], **Jessica A. Pfeilsticker**, **K. Barry Sharpless**[§], and **James R. Heath**[*]

Nanosystems Biology Cancer Center: Division of Chemistry and Chemical Engineering, MC-127-72, California Institute of Technology, Pasadena, California 91125

[†]Division of Health Sciences and Technology, Massachusetts Institute of Technology, 77 Massachusetts Avenue, Cambridge, MA 02139

[‡]Integrated Diagnostics, 6162 Bristol Parkway, Culver City, CA 90230

[§]Department of Chemistry and The Skaggs Institute for Chemical Biology, The Scripps Research Institute 10550 North Torrey Pines Road, La Jolla, CA 92037 (USA)

[1]Institute of Bioengineering and Nanotechnology, 31 Biopolis Way, The Nanos, Singapore 138669

## Abstract

We describe the use of iterative in situ click chemistry to design an Akt-specific branched peptide triligand that is a drop-in replacement for monoclonal antibodies in multiple biochemical assays. Each peptide module in the branched structure makes unique contributions to affinity and/or specificity resulting in a 200 nM affinity ligand that efficiently immunoprecipitates Akt from cancer cell lysates and labels Akt in fixed cells. Our use of a small molecule to pre-inhibit Akt prior to screening resulted in low micromolar inhibitory potency and an allosteric mode of inhibition, which is evidenced through a series of competitive enzyme kinetic assays. To demonstrate the efficiency and selectivity of the protein-templated in situ click reaction, we developed a novel QPCR-based methodology that enabled a quantitative assessment of its yield. These results point to the potential for iterative in situ click chemistry to generate potent, synthetically accessible antibody replacements with novel inhibitory properties

## INTRODUCTION

A critical bottleneck in the transition from a potential cancer biomarker to a clinical diagnostic tool is the availability of high-affinity, high-selectivity molecular entities to recognize and capture biomarkers from complex biological mixtures. Almost all current platforms employ antibodies as capture agents despite their high cost, poor stability[1,2], and the batch-to-batch variability that often characterizes biologicals. Many antibodies are poorly characterized and reports have called into question the high specificity that is a perceived hallmark of antibodies[3,4]. Developing protein capture agent approaches, such as

[*]Corresponding Author: Nanosystems Biology Cancer Center: Division of Chemistry and Chemical Engineering, MC-127-72, California Institute of Technology, Pasadena, California 91125.

**Author Contributions**
All authors have given approval to the final version of the manuscript.

Supporting Information. Full citations for references 6 and 28, synthetic protocols, compound characterization, experimental protocols, and additional data. This material is available free of charge via the Internet at http://pubs.acs.org.

phage display peptides[5] or nucleic acid aptamers can potentially represent a powerful alternative to antibodies for certain diagnostic arrays[6,7]. However, the challenge of finding a general and robust approach to produce protein capture agents that match the performance of monoclonal antibodies remains daunting. An ideal antibody replacement would be synthetically facile, stable to a range of thermal and chemical conditions, and display high affinity and specificity for the target of interest.

A high quality monoclonal antibody possesses a low-nanomolar affinity and high target specificity. Interestingly, structural and genetic analyses of the antigen recognition surface have shown that the majority of the molecular diversity of the variable loops is contained in a single highly variable loop (CDR-H3)[8]. In humans, this loop ranges in size from 1-35 residues (15 on average)[9], can adopt a wide range of structural conformations[10], and is responsible for most of the interactions with the antigen molecule. The other five loops are significantly less diverse and adopt only a handful of conformations. This suggests that a carefully selected “anchor” peptide can dominate the mode and strength of a multiligand interaction. It also suggests that other peptide components, while providing only modest contributions to the total interaction energy, can supply important scaffolding features and specificity elements. Analogously, the iterative in situ click chemistry approach utilized here begins with an initial short-chain anchor peptide, and then proceeds by adding additional, covalently coupled peptide branches via a process that is promoted by the target protein. The specificity and inhibitory potency of the original anchor are augmented in the final multiligand by the peripheral peptide branches.

We recently reported on the technique of iterative in situ click chemistry for the production of a triligand capture agent against the model protein carbonic anhydrase II (CAII)[11]. The approach built upon the method of in situ click chemistry[12], which is a technique in which a small molecule enzymatic inhibitor is separated into two moieties, each of which is then expanded into a small library - one containing acetylene functionalities, and the other containing azide groups. The enzyme itself then assembles the ‘best fit’ inhibitor from these library components by selectively promoting the 1,3-dipolar cycloaddition between the acetylene and azide groups to form a triazole linkage (the ‘click’ reaction). The enzyme promotes the click reaction only between those library components that bind to the protein in just the right orientation. The resultant inhibitor can exhibit far superior affinity characteristics relative to the initial inhibitor that formed the basis of the two libraries[13,14]. Iterative in situ click chemistry extends this concept to enable the discovery of multiligand protein capture agents, and it has several advantages. First, structural information about the protein target is replaced by the ability to sample a very large chemical space to identify the ligand components of the capture agent. For example, an initial ligand binder (an anchor ligand) may be identified by screening the protein against a large ($> 10^6$ element) one-bead-one-compound (OBOC)[15] peptide library, where the peptides themselves may be comprised of natural, non-natural, and/or artificial amino acids. That anchor ligand is then utilized in an in situ click screen, again using a large OBOC library, to identify a biligand binder. A second advantage is that the process can be repeated, so that the biligand is used as an anchor to identify a triligand, and so forth. The final capture agent can then be scaled up using relatively simple and largely automated chemistries, and derivatized with biochemical handles, such as biotin, as an intrinsic part of its structure. The approach permits the exploration of branched, cyclic, and linear capture agent architectures. While many strategies for protein-directed multiligand assembly have been described[16,17], most require detailed structural information on the target to guide the screening strategy, and most (such as the original in situ click approach), are optimized for low-diversity small molecule libraries.

Here we extend the use of iterative in situ click chemistry to synthesize a high-specificity branched, triligand capture agent/inhibitor for the Akt kinase. Akt is a critical molecular router that mediates signal transduction from the plasma membrane (cytokine receptors, GPCRs) to downstream effector molecules that control cell growth, apoptosis, and translation[18]. Akt overexpression and/or hyperactivation has been observed in numerous cancer types[19]. Such ubiquitous and aberrant Akt activity has made Akt a target for cancer diagnostics and therapeutics[20]. For developing a capture agent/inhibitor against Akt, we developed two novel screening strategies. First, we report on the use of a pre-inhibit form of the kinase as a screening target, which provides an approach towards developing an allosteric site inhibitor. Second, we take advantage of the fact that an in situ click screen in which an anchor ligand and protein target are screened against a large OBOC library will selectively generate triazole-linked products on the hit beads. We characterize the efficiency of this process through the use of a novel QPCR assay to quantify the on-bead product. We also expand this concept in the form of 'product screens', in which the presence of on-bead clicked product is taken to be the signature of a hit bead. We show that such a product screen can be utilized to increase the affinity and/or selectivity of the final multiligand capture agent. Finally, we report on the affinity, selectivity, and inhibitory characteristics of the triligand capture agent/inhibitor, and we demonstrate its use in cell-based biological assays.

## EXPERIMENTAL SECTION

There are a number of affinity, selectivity, biochemical, and biological assays described in this work. Full experimental procedures, synthetic protocols, and additional experimental data are discussed, in detail, in the Supporting Information.

Three different types of screens were employed for this work. The first screen, called a target screen, is analogous to most screening strategies described in the literature. Hit beads are identified by selecting those beads onto which the target protein has bound. The second type of screen, called an inhibited target screen, is based on selecting those beads on to which to which the target protein has bound, but the screen itself is carried out in the presence of a small molecule inhibitor. The third type of screen is the above-described product screen; hit beads are identified by the presence of on-bead triazole-linked product.

### Screening: General

All screens utilized OBOC peptide libraries that were synthesized on TentaGel (Rapp Polymere) using standard Fmoc SPPS protocols. Blocking conditions were carried out in Akt Blocking Buffer: 25 mM Tris-Cl (pH = 7.5), 150 mM NaCl, 10 mM MgCl2, 0.1% (v/v) β-mercaptoethanol, 0.1% (v/v) Tween-20, and 1 mg/mL BSA. The results of each screen are presented in the Supporting Information.

### Screening: Anchor Ligand

An initial anchor ligand against Akt was identified through the use of an inhibited target screen. The OBOC library was synthesized manually, and was of the form $H_2$N-AzX-XXXXX-GYM-TG where TG = TentaGel resin, X = one of 18 natural L-amino acids (-Cys, -Met) and AzX = one of three azido amino acids Az2, Az4, and Az8 (Supporting Information, Figure S2). The syntheses of Az2 is described in the Supporting Information; the synthesis of Az4, and Az8 were carried out as previously described[11]. *Inhibited Target Screen*: The initial screen was carried out in the presence of 21 nM Akt1-S473E-T308P and 500 μM of the inhibitor Ac7 under blocking conditions for 75 min at room temperature. Binding was detected by probing with a monoclonal anti body specific for phosphorylated T308, followed by anti-mouse secondary antibodies conjugated with alkaline phosphatase.

Purple “hit” beads (defined by color change in the presence of 5-bromo-4-chloro-3-indolyl-phosphate/nitro blue tetrazolium (BCIP/NBT) substrate) were washed in water, stripped with 7.5 M Guad-Cl (pH = 2), and sequenced by Edman degradation (Supporting Information, Figure S3). The initial hit sequences defined a focused library which was subjected to an inhibited target screen as described above (Supporting Information, Figures S4 and S5). Candidate sequences were scaled up and tested for their ability to inhibit Akt1-S473E-T308P activity. The most potent sequence was re-synthesized as a C-terminal biotinylated peptide and used as the anchor in the biligand screen (Scheme 1).

### Screening: Biligand Branch

The biligand branch was identified through a two-step screening process of a target screen to identify potential hits, followed by a product screen of those hit beads to identify true hits. *Target Screen*: A naïve library of the form $H_2N$-Pra-XXXXX-GM-TG where TG = TentaGel resin, X = one of 18 natural L-amino acids (-Cys, -Met), and Pra = L-propargylglycine was synthesized by standard split-mix protocols on a Titan 357 automated peptide synthesizer (AAPPTEC). The library was incubated with 90 μM biotinylated anchor peptide and either Akt1-S473E (9 nM) or Akt1-S473E-T308P (37 nM) under blocking conditions for 90 min at room temperature. Binding was detected by antibodies against the phosphorylated or non-phosphorylated form of Akt1. After color development, purple hit beads were stripped, decolorized in DMF, and re-probed with the primary and secondary antibodies in the absence of target protein. Beads that remained clear were washed and stripped prior to the product screen. *Product Screen*: The beads were re-blocked and incubated with streptavidin-AlexaFluor647 (Invitrogen) at a concentration of 0.4 μg/mL for 30 minutes at room temperature. The beads were washed exhaustively with Akt Blocking Buffer and imaged on an Axon Genepix 4400A scanner (MDS). The beads displaying saturated fluorescence signal in the product screen were sequenced by Edman degradation (Supporting Information, Figure S8).

### Screening: Triligand Branch

The triligand branch was identified solely through a product screen. The initial naïve library was the same as in the initial anchor screen. The naïve library (100 mg) was pre-cleared against alkaline phosphatase-conjugated streptavidin (SA-AP), developed with BCIP/NBT, and the purple beads removed from the pool. The remaining library was stripped overnight, decolorized with NMP, and blocked. Akt biligand was synthesized with a C-terminal biotin and a 5-hexynoic acid cap and used as the anchor compound for the tertiary ligand screen (5HA-Biligand-Bio, Supporting Information, Figure S9). Product Screen: The 5HA-Biligand-Bio was incubated in the presence of the library at a concentration of 30 μM along with Akt-S473E at a concentration of 110 nM for 90 min at room temperature. The beads were washed as before, probed with SA-AP, developed in BCIP/NBT, and the purple beads were sequenced by Edman degradation (Supporting Information, Figure S10). A focused library (30 mg) based on the first round hit sequences was pre-cleared against SA-AP and subjected to a second round of product screening. The beads were developed in the presence of BCIP/NBT and the purple beads sequenced by Edman degradation (Supporting Information, Figure S11).

### QPCR-based assay for quantitating in situ click efficiency

The secondary peptide ($H_2N$-Pra-FWFLRG) and the anchor peptide ($H_2N$-Az8-VFYRLGY) were synthesized on TentaGel. 0.45 mg (~1000 beads) of each were combined with Akt-S473E (22 μM) and the corresponding biotinylated peptide (200 μM), the biotinylated peptide alone (200 μM), or DMSO. The Cu+-catalyzed click reaction contained 0.45 mg immobilized peptide, the biotinylated peptide (200 μM), CuI (9 mM), L-ascorbic acid (30 mM), and Tris[(1 - benzyl - 1H - 1,2,3 - triazol - 4 - yl)methyl] amine (TBTA, 4 mM) in a

final volume of 50 μL 4:1 NMP:dH2O. For immobilized secondary peptide, the corresponding soluble biotinylated peptide was Ac-Az8-VFYRLGY-Biotin. For immobilized anchor peptide, the corresponding soluble biotinylated peptide was Ac-Pra-FWFLRG-Biotin.

After incubating the in situ click reactions at 25 °C for 18 hr with strong agitation, the beads were removed and washed exhaustively in Akt Blocking Buffer. The Cu+ reactions were washed three times with NMP, ten times in copper chelation solution (22 mM sodium diethylthio carbamate (trihydrate), 29 mM DIEA, in DMF), three times in NMP, three times in water, and once in Akt Blocking Buffer. The beads were then stripped in 7.5 M Guad-HCl (pH = 2), washed in $dH_2O$, and blocked in QPCR Blocking Buffer for 2 hr. (0.3% (w/v) BSA, 0.1% (v/v) Tween-20, 150 μg/mL sheared salmon sperm DNA (Ambion) in phosphate buffered saline). The beads were then probed with 0.5 μg/mL streptavidin-oligonucleotide (SA-oligo) for 1 hr at room temperature. The beads were washed five times in QPCR Blocking Buffer and three times in PBS. Three sets of five beads for each reaction condition were placed in PCR tubes and subjected to QPCR on an Applied Biosystems 7300 instrument. Additional experimental details can be found in the Supporting Information.

## RESULTS AND DISCUSSION

The Akt1 kinase domain used here contained a S473E mutation which mimics phosphorylation at the critical S473 residue[21]. Expression of the kinase in insect cells (Hi5) produced ~ 20 mg/L of partially active enzyme (Akt1-S473E) as well as a small amount of fully active kinase phosphorylated at Thr308 (Akt1-S473E-T308P). Both were readily separated by anion-exchange chromatography, were enzymatically active, and were used as screening targets.

### In situ Click Screens

The sequential in situ click chemistry strategy begins with the identification of an anchor ligand. Although the anchor ligand can have low affinity for the target, the nature of how it binds to the target is likely the factor that most influences the rest of the multiligand development process. The dominant hot spot on Akt is the catalytic site which contains the ATP and peptide substrate binding sites. These sites and the catalytic residues provide the standard epitope for most kinase inhibitors. We hypothesized that blocking the ATP-binding site with a small molecule inhibitor (Scheme 1) would remove it as a thermodynamic sink for library binding. A second possibility, that wasn't observed, was that the kinase would direct the conjugation of the acetylene-bearing small molecule and the anchor peptide to form a bivalent inhibitor similar to those previously described[22,23]. The absence of the *in situ* click reaction between these components may be attributable to suboptimal proximity and/or spatial arrangement on the protein surface.

Our initial screen against Akt1-S473E-T308P generated a set of hits which informed the design of a focused library. Upon screening, this library yielded a set of highly similar sequences (Supporting Information, Figure S5). Interestingly, one of these peptides (Az8-VFYRLGY-$CONH_2$) showed almost 95% inhibition of the Akt1 kinase in the absence and presence of the conjugated small molecule inhibitor (Supporting Information, Figure S6). This peptide showed little resemblance to any known Akt1 peptide substrate[24] (e.g. RPRAATF), and was not phosphorylated by Akt in vitro (Supporting Information, Figure S7). The Ac7-independent inhibitory potency of the peptide suggested a novel mechanism for binding and inhibition which led us to employ it as an anchor for biligand development.

OBOC libraries have been previously employed to isolate protein kinase substrate sequences[25] as well as low affinity inhibitors for non-protein kinases[26]. However, we are

unaware of previous attempts to select an inhibitory peptide for a protein kinase in the presence of an ATP-competitive small molecule. Inhibition of kinases by ligands that bind outside the substrate sites is a well-known phenomenon and so the approach reported here may have some generality for the development of inhibitors[27]. Given the structural conservation of the ATP-binding pocket across kinases, and hence the often-observed poor selectivity of inhibitors targeted to such sites[28], an approach towards developing off-site inhibitors may have unique advantages.

While the anchor peptide displayed excellent selectivity for Akt1-S473E, its affinity (>25 μM) was unsuitable for high-sensitivity capture of Akt. To increase the affinity, a biligand branch was selected through a sequence of target and product screens (Scheme 2). For these screens the anchor peptide was modified with a C-terminal biotin for use in the product screen. We hypothesized that the combination of an initial target screen, followed by a product screen of those initial hit beads, would identify only the library members that bound the target and participated in a successful click event. The target screens resulted in hit frequencies between 0.001%–0.01% of the beads in the naïve library. The product screen with fluorescent streptavidin validated between 23%–37% of these beads for sequencing.

The sequences obtained in the secondary ligand screen showed a preference for aromatic amino acids in the first three random positions (Supporting Information, Figure S8). We selected three peptide sequences, and synthesized the corresponding biligands with the 1,4-triazole using the Cu(I)-catalyzed azide-alkyne cycloaddition[29,30]. Two of the three showed increased binding to Akt1 in immunoprecipitation experiments and the most promising candidate (Ac-Pra-FWFLRG-$CONH_2$, Pra = propargylglycine) was scaled up for additional characterization and for the development of the triligand.

For triligand development, the selected biligand was appended with 5-hexynoic acid at the N-terminus and used as the anchor ligand (Supporting Information, Figure S9). We omitted the target screen in these experiments, electing to employ only the product screen for triazole formation. Results from the naïve library revealed weak consensus for the tertiary peptide, although Az8 was the preferred amino acid at position 1, and positions 2, 3, and 4 showed a propensity for positively charged amino acids (Supporting Information, Figure S10). We designed a focused library based on the amino acid frequencies observed in the initial screen and identified a tertiary ligand consensus sequence with positively charged amino acids at positions 2 and 4, negatively charged amino acids at position 3 and hydrophobic amino acids at position 5 (Supporting Information, Figure S11). From this pool, we selected the tertiary peptide Ac-Az8-RHERI-$CONH_2$ and conjugated it to the biligand to form a biotinylated branched triligand (Figure 3A).

## Characterizing the On-bead In situ Click Reaction

The target screen is an important and unique aspect of the methodologies reported here. Thus, we sought to determine the efficiency and selectivity of the in situ click reaction between the on-bead secondary peptide and the soluble anchor peptide in the presence and absence of Akt1-S473E. Previous work in our laboratory[11] suggested that the in situ reaction is low-yielding relative to the Cu(I) catalyzed process. Thus, we developed an analytical assay based on Immuno-PCR[31] as a means of amplifying and detecting the in situ product. This method takes advantage of the exquisite sensitivity and large dynamic range of Quantitative PCR (QPCR). We carried out variations of the in situ click reaction between the biotinylated anchor peptide and resin-bound secondary peptides. We then used the biotin label to attach a streptavidin-oligonucleotide (SA-Oligo) onto only those beads that contained biligand product. In order to account for variable sizes, five beads were individually selected and added to each QPCR reaction, the threshold cycle (Ct) was determined for each reaction condition, and a standard curve was used to calculate the

amount of biligand present on the bead for each reaction condition (Figure 1). The click reaction between the two peptides was approximately 10-fold more efficient in the presence of Akt1 than in its absence, confirming the requirement for the target protein to catalyze the click reaction. When the anchor peptide was immobilized and the biotinylated secondary peptide was in solution, the efficiency of the in situ click process was reduced by a factor of four (but still above background level), suggesting that the in situ click reaction observed in the screen is dependent on the identities of the anchor and secondary peptides and the manner in which they are displayed (on-bead or in solution). The copper catalyzed click reaction did not display any orientation dependence, providing further evidence that the click reaction observed in the screening process is highly target-dependent.

The biligand branch was selected in the context of an 8-carbon linker between the two peptide ligands. We assayed for the selectivity of the in situ click screen by measuring the inhibition characteristics of biligands prepared with 1, 4, or 8 carbon atom linkers, but otherwise identical peptide components (Figure 2A). We found that the selected biligand with the longest linker (n = 8) possessed a significantly higher inhibitory potency (Figure 2B) relative to n=4 and n=1 linkers. This again suggests that the secondary peptide was selected in the context of spatial constraints that define the protein-peptide interactions. We note that only multiligands linked by 1-4 triazoles (anti) were synthesized. The in situ reaction can result in formation of both the 1-4 (anti) and 1-5 (syn) triazole. It is possible that the 1-5 triazole (syn) may be the favored linkage and may confer additional affinity and/or selectivity to the multiligand. However, based on the fact that our linker between the separate peptide ligands is a flexible eight-carbon bridge, we would not expect a significant difference between the two triazole isomers.

Taken together, these experiments suggest that the “hit” sequences that emerged from our biligand screens were determined by 1) the target protein, 2) the soluble anchor peptide and 3) the relative spacing between the azide and acetylene functionalities in each component. Since the signal-to-noise ratio of the in situ screen (true hit/false positive) depends on the relative rates of the target-mediated and background reactions, QPCR-guided optimization of the screening conditions may significantly increase the robustness of the sequential in situ click approach. In contrast to previous work with small molecule biligands[12,32,33], we expect the high conformational entropy of the anchor and secondary peptides to result in a smaller population of ternary complexes with the correct conformational and geometrical orientation required by the cycloaddition reaction. The use of long, conformationally restricted linkers in the anchor and library peptides, or perhaps the use of N-methylated amino acids[34] in the OBOC libraries, may reduce this effect and capture more of the individual binding energies in the biligand product.

## Affinity and Specificity Characterization of Multiligand PCC Agents

We tested the affinity of the anchor, biligand, and triligand by ELISA with immobilized Akt-S473E (Figure 3B). As a detection agent, the biligand showed >100-fold improvement in its affinity for Akt relative to the anchor peptide while the triligand showed only a modest affinity gain (2–3 fold). When the triligand is employed as an immobilized capture agent, analysis by Surface Plasmon Resonance (SPR) confirms mid- to low-nanomolar affinity for Akt1-S473E ($K_D$ = 200 nM, Figure 3C). We next sought to address the specificity of the triligand for a panel of His-tagged protein kinases (Figure 3D). For these assays, the multiligands were used as immobilized capture agents for Akt1-S473E as well as a set of commercially available active, his-tagged protein kinase domains from the AGC family (Akt1, PDK1, and p70s6 kinase), the STE family (MEK1), and the GMGC family (GSK3β). The relative affinity of each kinase was determined by probing with a horseradish peroxidase-conjugated anti-His6 antibody and normalizing the response to Akt1-S473E. The anchor was very specific for the Akt1 protein, with only modest binding to GSK3β. The

significantly higher affinity biligand showed reduced selectivity, with significant cross-reactivity to GSK3β. For the triligand, however, binding to GSK3β was significantly reduced, bringing it close to the level observed for the anchor peptide. Additionally, the off-target binding to MEK1 is completely eliminated at the triligand stage. To quantify the changes in selectivity for Akt1 and GSK3β, we carried out a similar ELISA-based binding analysis using a range of kinase concentrations (Supporting Information, Figure S18). As we translate from biligand to triligand, the affinity for Akt1 increases modestly while the affinity for GSK3β is decreased by approximately 2-fold. This demonstrates that Akt1 specificity, which is lost at the biligand stage, is partially regained at the triligand stage, mainly through destabilizing interactions with GSK3β.

The biligand exhibited a significant affinity enhancement for Akt1, but also a reduced selectivity when assayed against off-target kinases. The triligand, by contrast, exhibited only a modest affinity improvement, but a significant selectivity enhancement relative to the biligand. These observations suggest that large increases in affinity may come at the cost of reduced specificity, but the increased specificity need not be accompanied by increased affinity. This is consistent with previous studies on antibody-small molecule interactions[35], DNA-protein interactions[36], and protein-protein interactions[37–39]. Indeed, a recent study demonstrated an inverse correlation between affinity and selectivity for small molecule protein kinase inhibitors[40]. For the case of the capture agents reported here, the tertiary peptide contributes destabilizing interactions to GSK3β while making only marginal stabilizing interactions to Akt1. This suggests that the in situ click product screen approach described here has the potential to increase the specificity of the multiligand in a manner reminiscent of negative design[41]. This makes intuitive sense. Unlike most screening methodologies, the product screening strategy employed here does not define hits as those that bind the protein most strongly, but instead it defines hits as those that are compatible with the protein-catalyzed process

## Triligand Inhibition of Akt1

We carried out two standard enzyme kinetic assays to determine the mode of Akt1 inhibition by the triligand[42]. For such assays, the kinase activity is measured under varying substrate and triligand concentrations (Figure 4). The resulting data can be interpreted so that the nature of the competition between the triligand and the substrate for the relevant kinase binding site is determined. For example, if the triligand and ATP competed for the same binding pocket, the maximum velocity ($V_{max}$) of the kinase would be unchanged while the Michaelis constant ($K_M$) would increase. The plots can also be used as a means of determining the inhibition constant ($K_i$), of the triligand. The results (Figure 4) show reduction in the enzyme $V_{max}$ for both substrates, as a function of increasing triligand concentration. This indicates that the triligand does not directly compete with either substrate for binding to their respective binding sites. When ATP is the varied substrate, triligand addition appears to have no effect on $K_M$, consistent with noncompetitive inhibition. When the peptide concentration is varied, $K_M$ decreases in a manner consistent with uncompetitive inhibition. However, when inhibition constants are determined from the Dixon plot (varied [ATP]) and the Cornish-Bowden plot (varied [peptide]), the similarity in values (4 μM vs. 2.6 μM respectively, Table 1) suggests that triligand inhibition occurs in a noncompetitive fashion. Regardless of the exact mechanism, these experiments rule out competitive inhibition with respect to the ATP and peptide substrates.

The competitive enzyme kinetics studies demonstrate that the triligand binds to a site distinct from the active (ATP or peptide-binding) site of the kinase, and so achieves its inhibitory characteristics via an allosteric mechanism. This supports our hypothesis that blocking the ATP-binding site with Ac7 enabled the library to sample alternate binding sites with unexpected functional properties. While the precise mechanism for inhibition is

unknown, competition ELISA experiments suggest that the multiligand binding site may partially overlap with that of an anti-Akt1 antibody directed toward the C-terminus (Supporting Information, Figure S17). The C-terminus is effectively on the ‘backside’ of the kinase domain, opposite the active site.

## Biological Applications of the Branched Triligand

The ultimate test of a protein capture agent is whether or not it can be used to detect its cognate protein from a biologically relevant sample. We tested whether the multiligand capture agents could recognize full-length Akt from cancer cell lines. Previous studies have shown that Akt2 is overexpressed in the OVCAR3 ovarian cancer cell line, and so we utilized this cell line as an experimental platform for immunoprecipitation (IP) and immunocytochemical experiments (ICC)[43]. For the IP experiments, we immobilized the anchor, biligand, and triligand on streptavidin-agarose and panned each resin with OVCAR3 cell lysates obtained from cells stimulated with a combination of epidermal growth factor (EGF) and insulin, or untreated cells (Figure 5A). Probing the elutions with pan-Akt antibody, which detects all three isoforms of Akt, confirms the increased affinity of the biligand relative to the anchor peptide in lysates from both induced and non-induced cells. The triligand shows somewhat increased immunoprecipitation of Akt relative to the biligand in induced cell lysates but not in the non-induced control cell lysate. This effect is also observed when the immunoprecipitations are probed with an antibody specific for Akt phosphorylated Ser473 (Ser474 in Akt2). Analysis of the total immunoprecipitated protein by SDS-PAGE showed low non-selective binding for all the ligands (Supporting Information, Figure S15). A protein at approximately 50 kDa is immunoprecipitated by the triligand, and to a lesser extent, by the anchor and biligand. Based on our characterization of triligand specificity, this likely corresponds to the GSK3 kinase which has a predicted molecular weight of 47 kDa. We are currently investigating the basis for off-target GSK3 binding which is particularly surprising given the low sequence homology between Akt1 and GSK3.

These experiments confirm the increase in capture efficiency as the combined affinity/selectivity metrics of the capture agent are increased by translating from anchor to biligand to triligand, particularly in cells stimulated through the PI3K pathway by insulin and EGF. We compared the performance of our capture agent against an antibody that was similarly raised against the kinase domain of Akt1 (Figure 5A, lane 5) for an ‘apples to apples’ comparison of immunoprecipitation efficiency. Interestingly, the commercial anti-Akt1 antibody shows almost no immunoprecipitation of Akt. The poor performance of the antibody may be due to non-optimal presentation on streptavidin-agarose, or some other experimental artifact, but that poor performance was observed across many assays, and across multiple batches of antibody. Even for an equivalently performing antibody, the ability to use large amounts of triligand at relatively low cost relative to a monoclonal antibody confers a significant advantage.

To further explore the interaction between the multiligand capture agent and full-length Akt, we synthesized a fluorescein-labeled triligand (Supporting Information, Figure S16) and employed it as an ICC imaging agent in fixed, permeabilized OVCAR3 cells. This construct was benchmarked against a fluorescein-labeled monoclonal antibody specific for Akt. For this assay, Akt is expected to locate to the cell membrane following stimulation of receptor tyrosine kinases by EGF and insulin. Images of unstimulated and stimulated cells clearly reveal this effect (Figure 5B). Both compounds show localization of Akt at the plasma membrane after cell stimulation, presumably mediated through binding of the pleckstrin homology domain (PHD) to Phosphatidylinositol (3,4,5)-trisphosphate at the inner face of the membrane.

## CONCLUSIONS

In this work we have demonstrated the design of a peptide-based drop-in replacement for Akt monoclonal antibodies using iterative on-bead in situ click chemistry. The triligand can function as both a capture and detection agent in standard ELISA and biological assays. The allosteric inhibitory properties of the triligand highlight an additional therapeutic potential of these novel capture agents that we are currently investigating.

## Supplementary Material

Refer to Web version on PubMed Central for supplementary material.

## Acknowledgments

**Funding Sources**

This work was supported by the National Cancer Institute grant No. 5U54CA119347 (J.R.H., P.I.), the Institute Collaborative Biotechnologies (contract no. W911NF-09-D-0001 from the U.S. Army Research Office), The Institute of Bioengineering and Nano-technology (Biomedical Research Council, Agency for Science, Technology and Research, Singapore), and the Grand Duchy of Luxembourg via a sub-contract from the Institute for Systems Biology. SWM acknowledges support from an NRSF postdoctoral fellowship 1F32CA136150-01.

We thank Prof. Carl Parker for the generous use of his equipment and expertise. The Akt1-S473E plasmid was a gift from Dr. Shoshana Klein (The Hebrew University of Jerusalem). Expression of the Akt1-S473E was carried out by the Protein Expression Center at Caltech.

## References

1. Borrebaeck CAK. Immunology Today. 2000; 21:379. [PubMed: 10916140]
2. Kodadek T, Reddy MM, Olivos HJ, Bachhawat-Sikder K, Alluri PG. Accounts of Chemical Research. 2004; 37:711. [PubMed: 15379586]
3. Kijanka G, IpCho S, Baars S, Chen H, Hadley K, Beveridge A, Gould E, Murphy D. Journal of Immunological Methods. 2009; 340:132. [PubMed: 18996391]
4. Michaud GA, Salcius M, Zhou F, Bangham R, Bonin J, Guo H, Snyder M, Predki PF, Schweitzer BI. Nat Biotechnol. 2003; 21:1509. [PubMed: 14608365]
5. Smith GP, Petrenko VA. Chem Rev. 1997; 97:391. [PubMed: 11848876]
6. Gold L, et al. PLoS One. 2010; 5:e15004. [PubMed: 21165148]
7. Ostroff RM, Bigbee WL, Franklin W, Gold L, Mehan M, Miller YE, Pass HI, Rom WN, Siegfried JM, Stewart A, Walker JJ, Weissfeld JL, Williams S, Zichi D, Brody EN. PLoS One. 2010; 5:e15003. [PubMed: 21170350]
8. Xu JL, Davis MM. Immunity. 2000; 13:37. [PubMed: 10933393]
9. Zemlin M, Klinger M, Link J, Zemlin C, Bauer K, Engler JA, Schroeder HW Jr, Kirkham PM. J Mol Biol. 2003; 334:733. [PubMed: 14636599]
10. Chothia C, Lesk AM, Tramontano A, Levitt M, Smith-Gill SJ, Air G, Sheriff S, Padlan EA, Davies D, Tulip WR, et al. Nature. 1989; 342:877. [PubMed: 2687698]
11. Agnew HD, Rohde RD, Millward SW, Nag A, Yeo WS, Hein JE, Pitram SM, Tariq AA, Burns VM, Krom RJ, Fokin VV, Sharpless KB, Heath JR. Angew Chem Int Ed Engl. 2009; 48:4944. [PubMed: 19301344]
12. Manetsch R, Krasinski A, Radic Z, Raushel J, Taylor P, Sharpless KB, Kolb HC. J Am Chem Soc. 2004; 126:12809. [PubMed: 15469276]
13. Jencks WP. Proc Natl Acad Sci U S A. 1981; 78:4046. [PubMed: 16593049]
14. Murray CW, Verdonk ML. J Comput Aided Mol Des. 2002; 16:741. [PubMed: 12650591]
15. Lam KS, Salmon SE, Hersh EM, Hruby VJ, Kazmierski WM, Knapp RJ. Nature. 1991; 354:82. [PubMed: 1944576]

16. Erlanson DA, Braisted AC, Raphael DR, Randal M, Stroud RM, Gordon EM, Wells JA. Proceedings of the National Academy of Sciences. 2000; 97:9367.
17. Shuker SB, Hajduk PJ, Meadows RP, Fesik SW. Science. 1996; 274:1531. [PubMed: 8929414]
18. Vivanco I, Sawyers CL. Nat Rev Cancer. 2002; 2:489. [PubMed: 12094235]
19. Altomare DA, Testa JR. Oncogene. 2005; 24:7455. [PubMed: 16288292]
20. Garcia-Echeverria C, Sellers WR. Oncogene. 2008; 27:5511. [PubMed: 18794885]
21. Klein S, Geiger T, Linchevski I, Lebendiker M, Itkin A, Assayag K, Levitzki A. Protein Expr Purif. 2005; 41:162. [PubMed: 15802234]
22. Meyer SC, Shomin CD, Gaj T, Ghosh I. J Am Chem Soc. 2007; 129:13812. [PubMed: 17944472]
23. Shomin CD, Meyer SC, Ghosh I. Bioorg Med Chem. 2009; 17:6196. [PubMed: 19674907]
24. Obata T, Yaffe MB, Leparc GG, Piro ET, Maegawa H, Kashiwagi A, Kikkawa R, Cantley LC. J Biol Chem. 2000; 275:36108. [PubMed: 10945990]
25. Souroujon MC, Mochly-Rosen D. Nat Biotech. 1998; 16:919.
26. Samson I, Kerremans L, Rozenski J, Samyn B, Van Beeumen J, Van Aerschot A, Herdewijn P. Bioorganic & Medicinal Chemistry. 1995; 3:257. [PubMed: 7606387]
27. Kirkland LO, McInnes C. Biochem Pharmacol. 2009; 77:1561. [PubMed: 19167366]
28. Karaman MW, et al. Nat Biotechnol. 2008; 26:127. [PubMed: 18183025]
29. Rostovtsev VV, Green LG, Fokin VV, Sharpless KB. Angew Chem Int Ed Engl. 2002; 41:2596. [PubMed: 12203546]
30. Tornøe CW, Christensen C, Meldal M. The Journal of Organic Chemistry. 2002; 67:3057. [PubMed: 11975567]
31. Niemeyer CM, Adler M, Wacker R. Trends Biotechnol. 2005; 23:208. [PubMed: 15780713]
32. Mocharla VP, Colasson B, Lee LV, Roper S, Sharpless KB, Wong CH, Kolb HC. Angew Chem Int Ed Engl. 2004; 44:116. [PubMed: 15599912]
33. Whiting M, Muldoon J, Lin YC, Silverman SM, Lindstrom W, Olson AJ, Kolb HC, Finn MG, Sharpless KB, Elder JH, Fokin VV. Angew Chem Int Ed Engl. 2006; 45:1435. [PubMed: 16425339]
34. Chatterjee J, Gilon C, Hoffman A, Kessler H. Acc Chem Res. 2008; 41:1331. [PubMed: 18636716]
35. Schildbach JF, Panka DJ, Parks DR, Jager GC, Novotny J, Herzenberg LA, Mudgett-Hunter M, Bruccoleri RE, Haber E, Margolies MN. Journal of Biological Chemistry. 1991; 266:4640. [PubMed: 1999439]
36. Jen-Jacobson L. Biopolymers. 1997; 44:153. [PubMed: 9354759]
37. Nguyen JT, Porter M, Amoui M, Miller WT, Zuckermann RN, Lim WA. Chem Biol. 2000; 7:463. [PubMed: 10903934]
38. Nguyen JT, Turck CW, Cohen FE, Zuckermann RN, Lim WA. Science. 1998; 282:2088. [PubMed: 9851931]
39. Zarrinpar A, Park SH, Lim WA. Nature. 2003; 426:676. [PubMed: 14668868]
40. Posy SL, Hermsmeier MA, Vaccaro W, Ott K-H, Todderud G, Lippy JS, Trainor GL, Loughney DA, Johnson SR. Journal of Medicinal Chemistry. 2011; 54:54. [PubMed: 21128601]
41. Mason JM, Muller KM, Arndt KM. Biochemistry. 2007; 46:4804. [PubMed: 17402748]
42. Segel, IH. Enzyme kinetics : behavior and analysis of rapid equilibrium and steady state enzyme systems. Wiley; New York: 1975.
43. Yang L, Dan HC, Sun M, Liu Q, Sun XM, Feldman RI, Hamilton AD, Polokoff M, Nicosia SV, Herlyn M, Sebti SM, Cheng JQ. Cancer Res. 2004; 64:4394. [PubMed: 15231645]

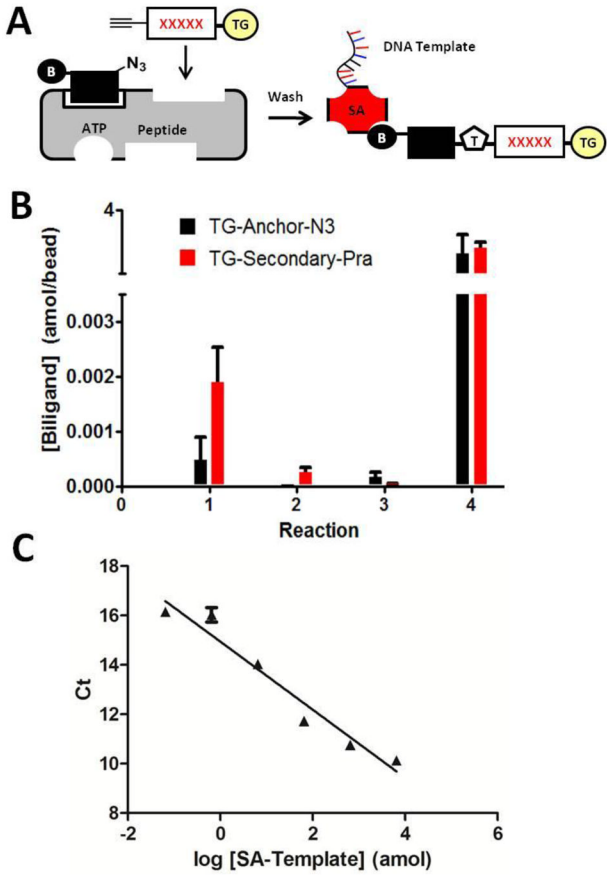


**Figure 1. Determination of On-bead In situ Click Reaction Efficiency**

(A) The secondary ligand (red letters) is synthesized on TentaGel (yellow) with an N-terminal propargylglycine and the soluble anchor peptide is appended with a C-terminal biotin (black) and an N-terminal azido-amino acid (Az8). These are incubated together under conditions described below. After the reaction is completed, the beads are washed, stripped, and probed with a streptavidin-oligonucleotide template (SA-Oligo) (red) to detect the formation of the triazole. The beads were then subjected to on-bead QPCR (B) Results of QPCR. The reaction conditions were (1) Akt1 + biotinylated anchor peptide + Bead, (2) Biotinylated anchor peptide + Bead, (3) Bead, and (4) CuI/Ascorbic Acid + biotinylated anchor peptide + Bead. The red bars represent the reaction configuration described in (a); the black bars represent reactions where the anchor peptide is synthesized on bead and the biotinylated secondary peptide is in solution (inverted configuration). The error bars represent standard error. In this experiment, the efficiency of the on-bead in situ click reaction is approximately 10-fold higher in the presence of the Akt1 target than in its absence. For comparison, the efficiency of the Cu(I)-catalyzed click reaction is approximately 4 orders of magnitude higher than the protein-templated reaction. (C) Standard Curve of SA-Oligo Template: Each point is the mean Ct of duplicate experiments

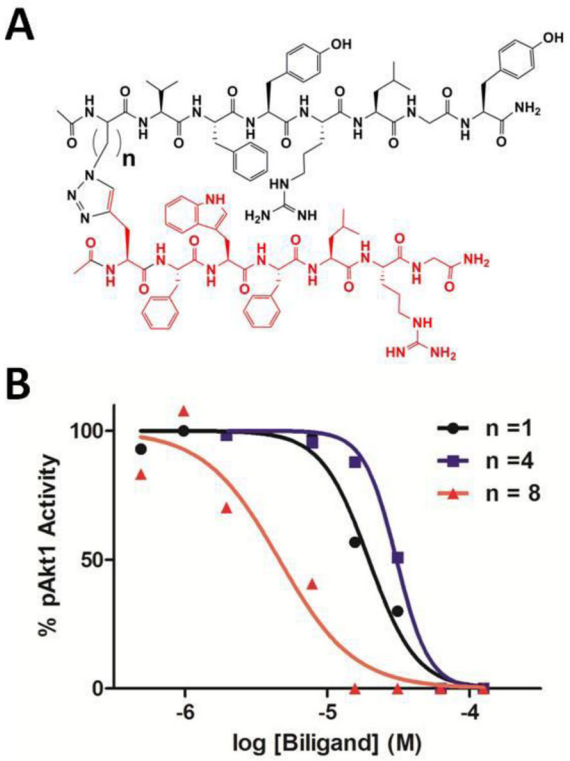


**Figure 2. Effect of Biligand Linker Length on Akt Inhibition**

(A) Biligands were synthesized with 1, 4, and 8 carbon linkers between the anchor peptide and triazole. (B) Each variant was titrated against activated Akt1-S473E-T308P, the activity was measured by immunoblotting, and quantitated by densitometry. The n = 8 linker which was present in the screen clearly yields the biligand with the highest inhibitory potency.

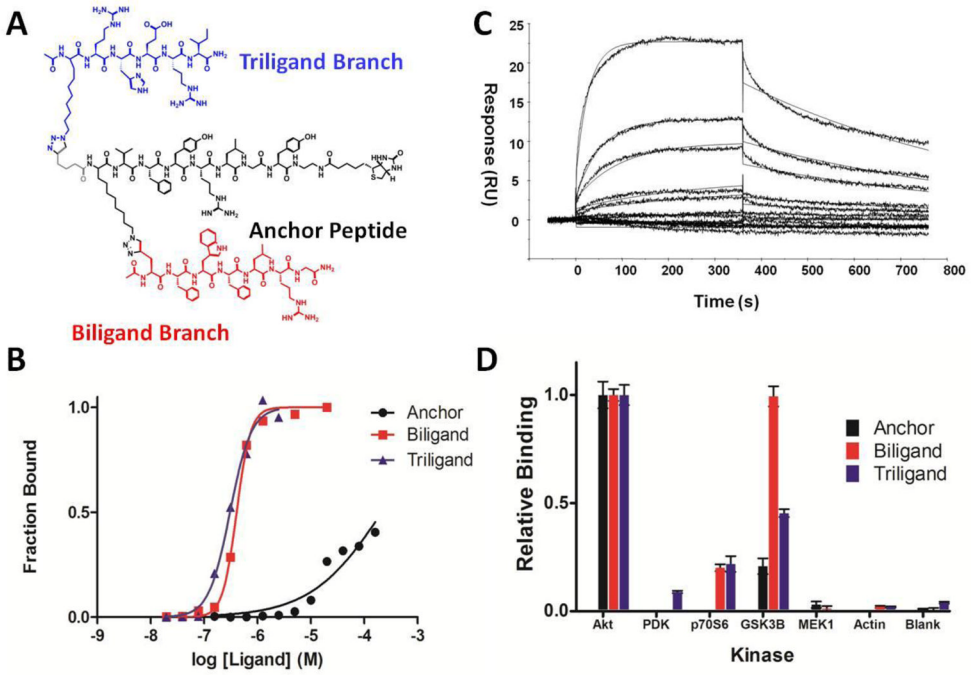


**Figure 3. Characterization of Akt Triligand**

(A) Structure of the biotinylated Akt Triligand (B) Relative affinity of Akt triligand and its components. Akt-S473E was immobilized on Ni-NTA plates and incubated with varying concentrations of biotinylated peptide. All values were normalized to the binding observed at saturation. (C) Absolute affinity of the triligand by surface plasmon resonance. For this experiment, the biotinylated triligand was immobilized on a streptavidin-derivatized Biacore chip and probed with Akt-S473E. Fits for the sensograms are shown as solid lines and the $K_D$ was found to be 200 nM by determination of the kinetic parameters. (D) Specificity of anchor, biligand, and triligand. Biotinylated ligand was immobilized on Streptavidin plates and probed with an array of His-tagged kinases. Values represent the mean A450 obtained from three experiments after normalization to Akt1-S473E binding. The error bars show the standard error. Note that although the affinity of the triligand is only marginally improved over the biligand, the selectivity for Akt1 is clearly enhanced.

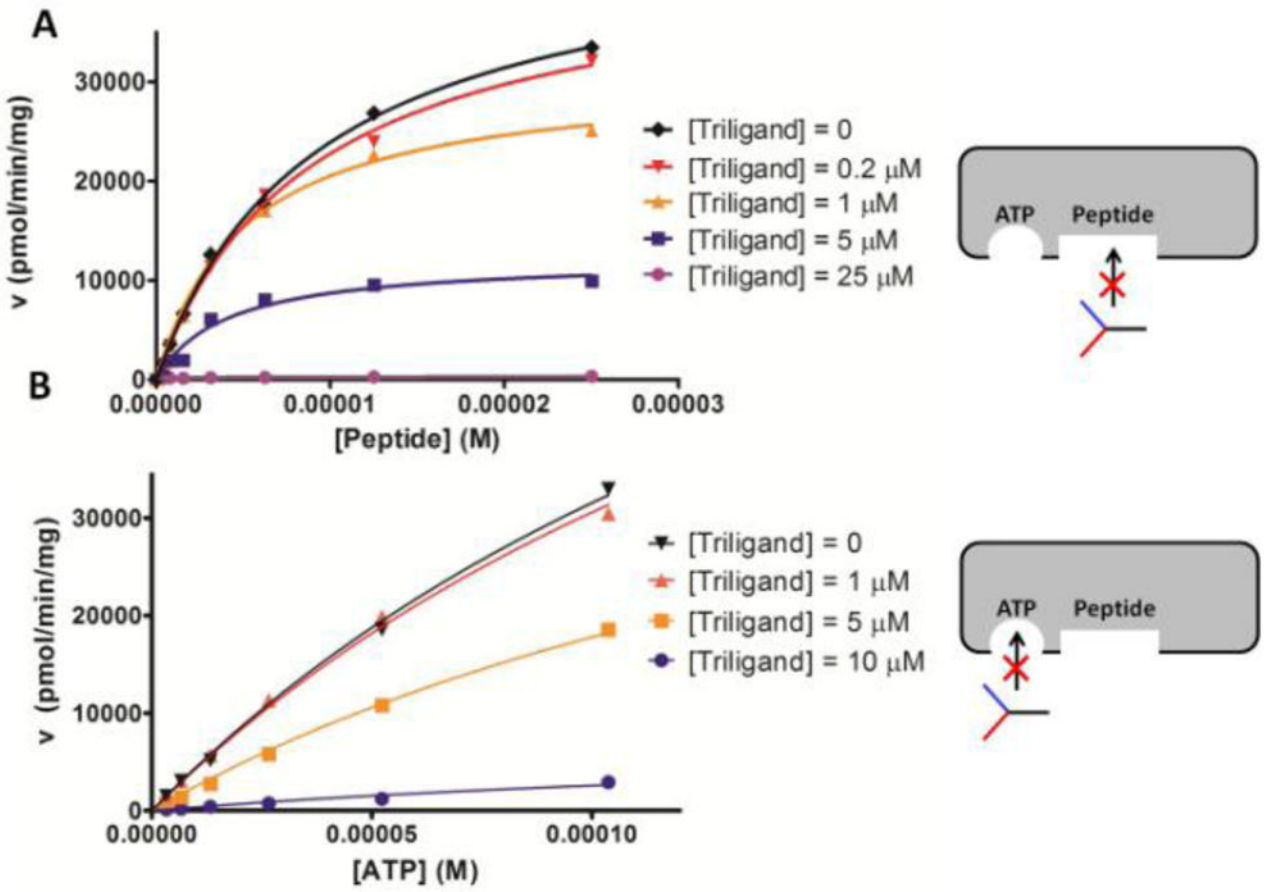


**Figure 4. Inhibition of Akt1 activity**

(A) Velocity vs. [Peptide substrate]with varying concentration of inhibitory triligand. (B) Velocity vs. [ATP] with varying concentration of inhibitory triligand. In both experiments, the $V_{max}$ of Akt1 is decreasing as the [Triligand] increases, evidence that the triligand is not competing with either substrate. The figures to the right of each graph illustrate the conclusion that the triligand was not competitive with respect to either the peptide or ATP binding site.

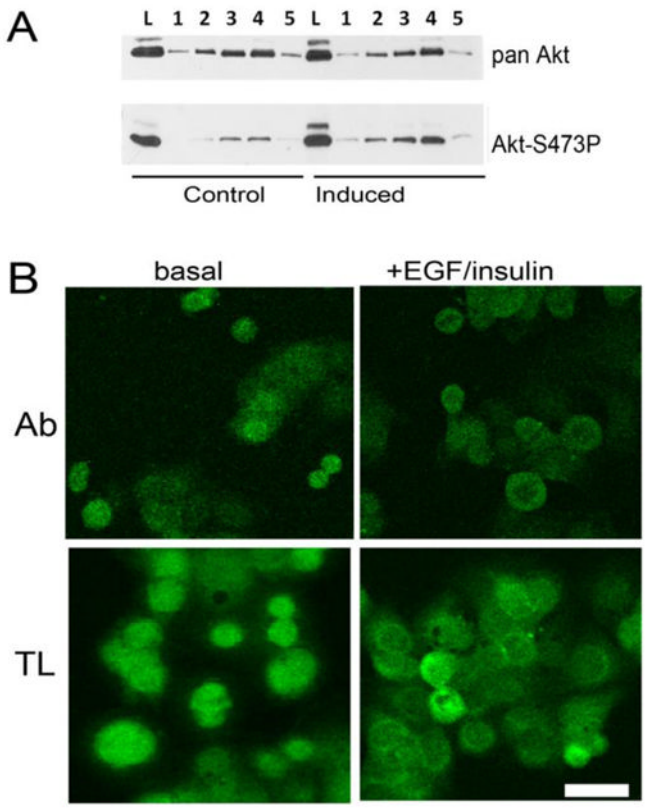


**Figure 5. Immunoprecipitation and Immunocytochemical Experiments with OVCAR3 Cells**

(A) Biotinylated ligands were immobilized on streptavidin-agarose and incubated with lysates from OVCAR3 cell lines treated with EGF and insulin (induced) or untreated (control). After 18 hr at 4 °C, resins were washed exhaustively, eluted with SDS-PAGE sample buffer, and analyzed by Western blotting. 1. Blank resin, 2. Anchor, 3. Biligand, 4. Triligand, 5. [5G3] mAb, L. lysate. (B) Immunofluorescent images of Akt in fixed OVCAR3 cells stained with either a fluorescein-conjugated anti-AKT antibody (Ab) or a fluorescein-conjugated triligand (TL). Each imaging agent distinguishes cytoplasmic or membrane-bound AKT in unstimulated or EGF+insulin- treated cells, respectively. Contrast is enhanced equally in all images but the fluorescence images of the triligand stained cells were achieved at a 3-fold lower excitation laser intensity relative to the (much dimmer) antibody-stained cells. Scale bar = 100 μm.

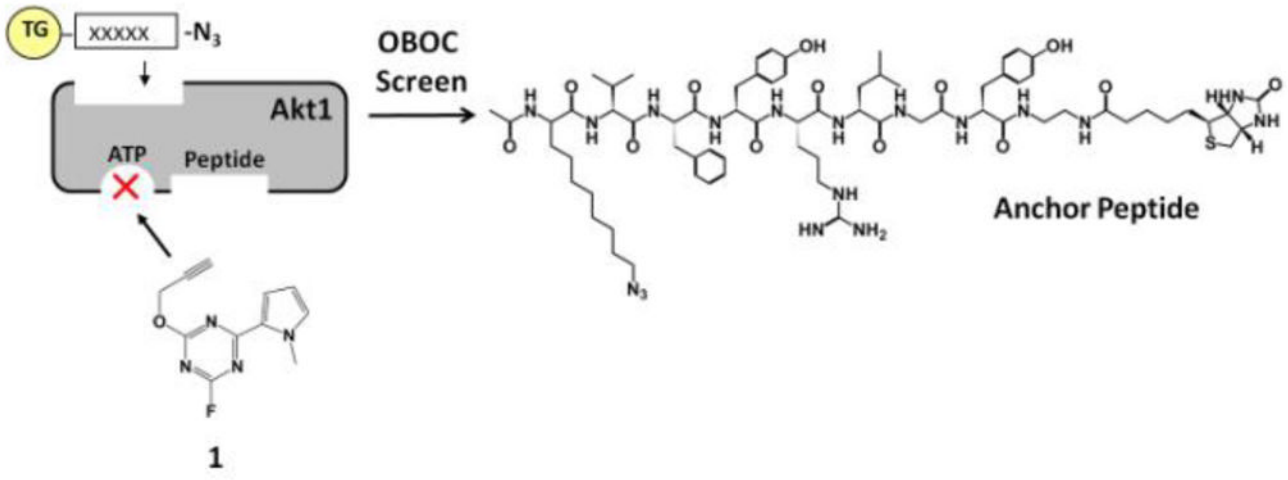


**Scheme 1. Selection of Anchor Peptide**

The kinase domain of Akt1 (*grey*) is pre-incubated with an ATP-competitive small molecule inhibitor, Ac7 (1). The inhibited kinase is then screened with a comprehensive solid-phase pentamer library on TentaGel (*yellow circle*) with an N-terminal azido-amino acid. The structure of the resulting biotinylated anchor peptide is also shown.

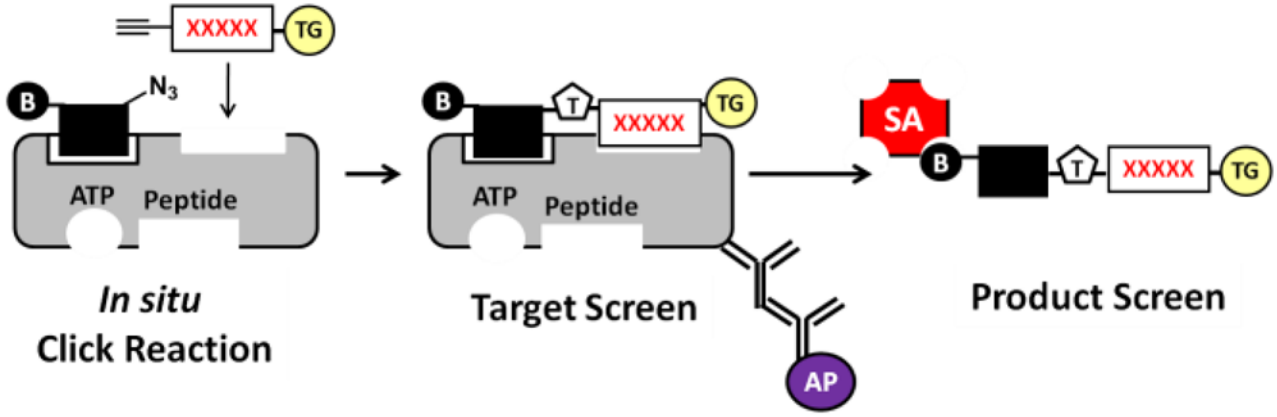


**Scheme 2. Strategy for Biligand Screens**

A comprehensive pentapeptide library is synthesized on TentaGel (*yellow circle*) and appended with propargylglycine, an acetylene-containing amino acid. This library is incubated with the Akt1 kinase domain (*grey*) and biotinylated anchor peptide (*black)*. The solid-phase library is probed with an anti-Akt antibody followed by a secondary antibody conjugated to alkaline phosphatase (*purple)*. Hit beads are re-probed with the antibodies alone to eliminate antibody binders. The hit beads are washed, stripped, and re-probed with AlexaFluor647-labelled streptavidin (*red*) and imaged for fluorescence. The most highly fluorescent beads are sequenced to obtain the biligand candidates. The target screens resulted in hit frequencies between 0.001%–0.01% of the beads in the naïve library while the product screen validated between 23%–37% of these beads for sequencing.

## Table 1
### Kinetic Parameters from Competition Experiments

$K_M$ and $V_{max}$ values for Akt1-S473E-T308P were obtained by nonlinear regression from the results of the inhibition experiments described above (GraphPad). The literature values for the Michaelis constants for ATP and substrate peptide were taken from Klein et. al.[21]. The triligand $K_i$ (noncompetitive inhibition) was obtained from the negative X-intercept of the Dixon plot of 1/v vs. [Triligand] with varying [ATP]. The $K_i$ is the mean value of the observed X-intercepts and the error range is the standard deviation. The triligand $K_i'$ (uncompetitive inhibition) was obtained from the intercept of the Cornish-Bowden plot of [peptide]/v vs. [Triligand] with varying [Peptide]. The $K_i'$ is the mean value of the intercepts and the error range is the standard deviation. These plots as well as additional kinetic analyses are presented in Supporting Information Figures S12 and S13.

| | V vs. [Peptide), Variable (Triligand) | V vs. [ATP], Variable [Triligand) |
|---|---|---|
| $K_M$(μM) (This work) | 9 +/− 0.7 (Peptide) | 213 +/− 25 (ATP) |
| $K_M$ (μM) (Literature] | 3.5 (Peptide) | 155(ATP) |
| $V_{max}$ (pmol/min/mg) | 45764 +/− 1486 | 98996 +/− 8242 |
| $K_i(K_i')$(μM) | (2.6 +/− 0.7) | 4 +/− 1 |
| Inhibition Mode | Uncompetitive | Noncompetitive |